

## Improved performance of heat pumps helps to use full potential of subsurface space for Aquifer Thermal Energy Storage

Bloemendal, Martin; Jaxa-Rozen, Marc; Rostampour Samarin, Vahab

**Publication date**

2017

**Document Version**

Final published version

**Published in**

Proceedings 12th IEA Heat Pump Conference 2017

**Citation (APA)**

Bloemendal, M., Jaxa-Rozen, M., & Rostampour Samarin, V. (2017). Improved performance of heat pumps helps to use full potential of subsurface space for Aquifer Thermal Energy Storage. In *Proceedings 12th IEA Heat Pump Conference 2017* Stichting HPC 2017.

**Important note**

To cite this publication, please use the final published version (if applicable). Please check the document version above.

**Copyright**

Other than for strictly personal use, it is not permitted to download, forward or distribute the text or part of it, without the consent of the author(s) and/or copyright holder(s), unless the work is under an open content license such as Creative Commons.

**Takedown policy**

Please contact us and provide details if you believe this document breaches copyrights. We will remove access to the work immediately and investigate your claim.



12<sup>th</sup> IEA Heat Pump Conference 2017



## Improved performance of Heat Pumps helps to use full potential of subsurface space for Aquifer Thermal Energy Storage

Martin Bloemendal<sup>a,b,\*</sup>, Marc Jaxa-Rozen<sup>a</sup>, Vahab Rostampour<sup>a</sup>

<sup>a</sup>Delft University of Technology, Delft 2628RN, The Netherlands

<sup>b</sup>KWR Watercycle Research Institute, Nieuwegein 3433 PE, The Netherlands

---

### Abstract

The application of seasonal Aquifer Thermal Energy Storage (ATES) contributes to meet goals for energy savings and greenhouse gas (GHG) emission reductions. Heat pumps have a crucial position in ATES systems because they dictate the operation scheme of the ATES wells and therefore play an important role in utilizing the storage potential of the subsurface.

In the Netherlands, suitable climatic and geohydrological conditions in combination with progressive building energy efficiency regulation have caused the adoption of ATES to take off, resulting in a situation where demand for ATES exceeds the available subsurface space in many urban areas. The most important aspects in this problem are A) the permanent and often unused claim resulting from static permits for ATES operation, and B) excessive safety zones around wells to prevent interaction between wells. Both aspects result in an artificial reduction of subsurface space for potential new ATES systems. Recent research has shown that ATES systems could be placed much closer to each other, and that a controlled/limited degree of interaction between them can actually benefit the overall energy savings of an entire area.

Two different simulation experiments were carried out to evaluate the effect of an adaptive permit capacity policy, as well as revised layout guidelines for ATES wells. Our solution provides a framework in which smaller distances between wells and adaptability of the permit volume plays a key role, to allow for optimal utilization of subsurface space for ATES and maximize GHG emission reduction. This paper shows how the total GHG emission reduction of an area can be increased by intensifying the use of the aquifer by allowing (some) interaction between ATES wells, which opens up unused but claimed subsurface space, and increase the number of heat pumps and ATES systems installed.

© 2017 Stichting HPC 2017.

Selection and/or peer-review under responsibility of the organizers of the 12th IEA Heat Pump Conference 2017.

Keywords: Heat pumps ; ATES

---

### 1. Introduction

Globally there is a strong drive to meet energy demand sustainably. Seasonal Aquifer Thermal Energy Storage (ATES) systems provide sustainable heating and cooling to buildings. The potential for using ATES systems depends both on climatic and hydrogeological conditions; combining these two conditions showed that the application of ATES has potential in many areas over the world [1], and is therefore expected to rise in the future. Although the potential of ATES systems is largely not yet deployed in many parts of the world, practical experience with ATES systems has been developed in several European countries and elsewhere [2-5].

---

\* Corresponding author. Tel.: +31625179849

E-mail address: j.m.bloemendal@tudelft.nl.

Particularly in the Netherlands, the number of ATEs systems has grown rapidly in the past decade, often alongside the (re)development of urban areas [6]. Building energy efficiency regulations have driven this increase in demand for ATEs, illustrated in Figure 1.

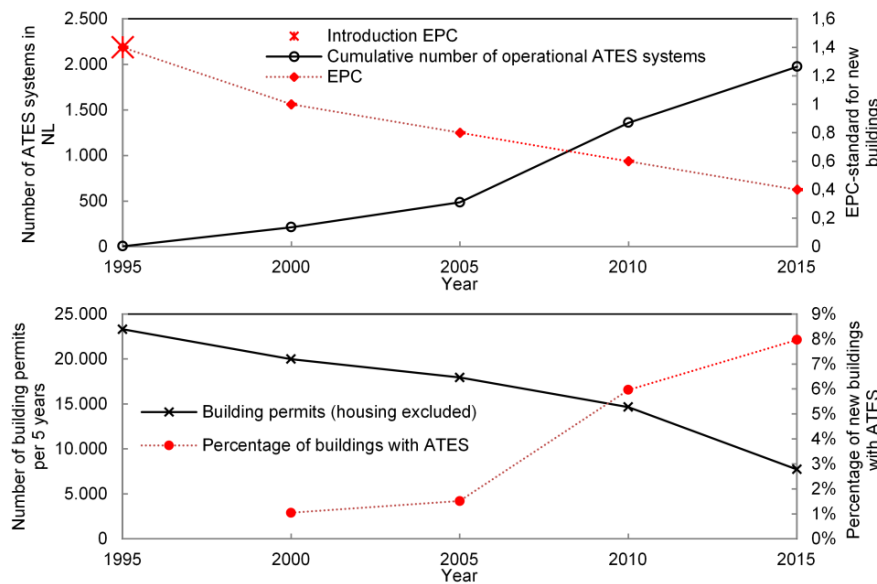


Figure 1. Top: number of ATEs systems in the Netherlands related to Energy Performance Coefficient (EPC) standard for houses; the EPC value reflects the expected energy use of a building, with EPC = 0 meaning no net energy use. Bottom: number of ATEs systems relative to new buildings constructed. [7-9].

ATEs systems are typically clustered in urban areas where many large buildings like offices and commercial areas are concentrated on top of a suitable aquifer. The spreading of warm and cold groundwater originating from the storage cycles depends on aquifer properties, ambient groundwater velocity and the energy demand of the associated buildings. Under typical conditions in the Netherlands, this spreading may vary in a radius between 20-150 m around the storage wells and, therefore, often crosses the plot of a building owner. As interaction between wells reduces the thermal efficiency of these systems, overlapping warm and cold zones are to be prevented.

However, the use of subsurface volume by ATEs wells is variable and hard to predict, due to uncertainties in energy demand caused by future weather conditions, climate and the use of the building – all of which influence ATEs operation. At the same time, the spreading of warm and cold groundwater in the subsurface is not visible and difficult and expensive to monitor. To prevent negative interaction of ATEs systems, they are over-dimensioned in current practice [6] and kept at a large distance between one and another [10]. This results in underutilization of subsurface volume, and a loss of potential greenhouse gas (GHG) savings with ATEs systems.

To maximize reduction of the emission of greenhouse gases by ATEs, it is crucial to minimize the claim on the subsurface by individual systems, to allow accommodation of the largest possible number of ATEs systems, while optimizing with respect to thermal recovery efficiency. As in many common-pool resource (CPR) problems [11], there is a trade-off between collective and individual performance; accommodation of more ATEs systems in an aquifer reduces the total GHG emissions of all the buildings in that area, while at the same time this may reduce the efficiency of individual systems [12]. In current practice, concerns over the latter prevail, which results in policies creating an artificial scarcity in the subsurface.

In that respect, although the energy performance of ATEs wells is important, some thermal losses in the subsurface may have limited effect on total GHG emission reductions of ATEs system due to the use of heat pumps for heat delivery [13]. This would relax the trade-off challenge between individual ATEs owners and the combined energy savings of all buildings in an area/city. In this paper, we challenge how the subsurface interactions affect the energy performance of ATEs systems. As such, the goal of this paper is to show how the total GHG emission reduction of an area can be increased by intensifying the use of the aquifer by allowing (some) interaction between systems. This may open up unused but claimed subsurface space, and increase the number of heat pumps and ATEs systems installed. From this perspective, two different simulation experiments

are carried out to evaluate the effect of an adaptive permit capacity policy, as well as revised layout guidelines for ATES wells.

This introduction is concluded by a short description of the working principle of ATES. The second section describes methods and materials, and is followed by simulation experiments, a discussion of the results, and conclusions as well as directions for future work.

### 1.1. Working principle of ATES

The basic principle of ATES is its use of the subsurface to overcome the discrepancy between the availability and demand for thermal energy. Buildings in moderate climates generally have a heat surplus in summer and a heat shortage in winter. Where groundwater is present in sandy layers of sufficient thickness and hydraulic conductivity, thermal energy can be stored in and extracted from the subsurface. An ATES system most often consists of one or more pairs of tube wells that infiltrate and simultaneously extract groundwater to store and extract thermal energy. They do so by changing the groundwater temperature through a heat exchanger that is connected to the associated building (Figure 2).

Buildings can be efficiently cooled in summer using the capacity of groundwater from the cold well to take up heat. The groundwater (which is warmed to 14-18°C when passed through the heat exchanger) is then stored by injection in the warm well. In winter, the same groundwater is extracted from the warm well for heating; the heat exchanger between the groundwater and the building circuit is accompanied by a heat pump, in order to raise the temperature in the water of the building circuit to a level which is suitable for heating. While doing so, the heat exchanger lowers the groundwater temperature to around 5-8 °C, making it suitable for subsurface storage in the cold well and use for cooling during the next summer.

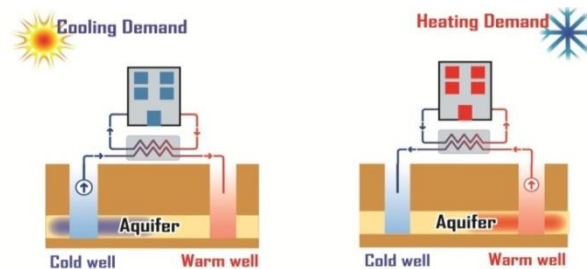


Figure 2. Principle of open geothermal energy storage system. Aquifer thickness in the Netherlands ranges from 10 to 160 m.

## 2. Methods and materials

### 2.1. Modeling environment

The problem described in section 1 can be understood as a complex adaptive system, due to the feedbacks and interactions between aquifer conditions and ATES/building operation. To simulate the development of ATES and the resulting performance trade-offs, this paper therefore relies on a coupled simulation architecture in which geohydrological dynamics are modelled using the MODFLOW / SEAWAT codes, while an agent-based model of ATES adoption and operation (detailed in [12]) is implemented using NetLogo. These model components are linked through an object-oriented architecture using the Python language. Figure 3 summarizes this architecture and the main exchanges of data across components. The coupled models are executed using the EMA<sup>†</sup> Workbench package for exploratory modelling [14], which allows for the generation of ensembles of experiments and for their analysis.

<sup>†</sup> Exploratory Modelling and Analysis

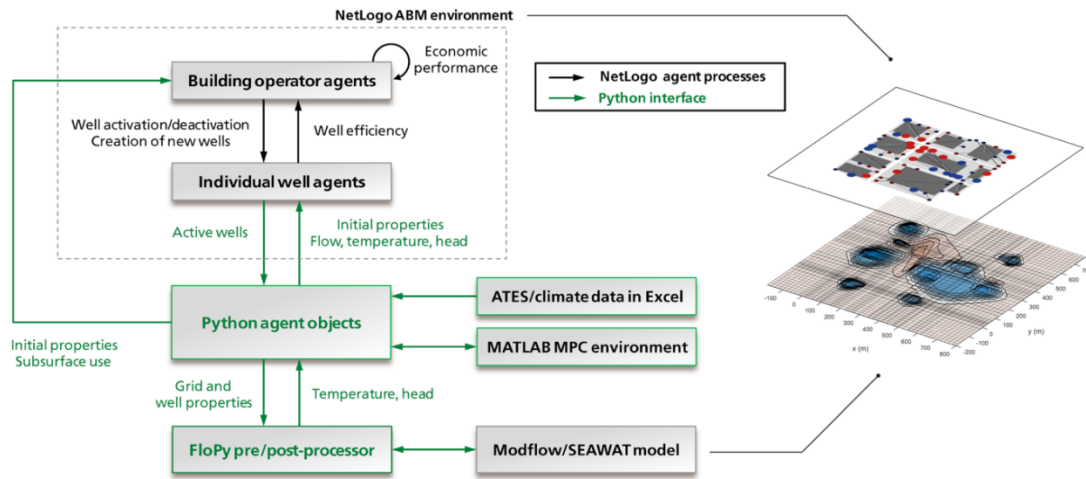


Figure 3. Coupled simulation architecture

## 2.2. Performance objectives

To represent the potential trade-off between individual and collective interests for ATEs operation, the main indicators used to assess ATEs performance are the aggregate operational cost savings of the simulated ATEs wells as well as the GHG savings realized, both relative to a conventional building energy system. Additional measures track the specific cost savings per cubic meter of water pumped by ATEs systems, and the specific GHG savings realized per cubic meter of subsurface space allocated to ATEs thermal zones. These measures provide an indication of the individual and collective efficiency of the systems.

The total GHG emissions saved are retrieved by calculating the CO<sub>2</sub> emissions of the ATEs systems (1 to  $N$ ) (Eq. (1)) and comparing those emissions with the emissions of a conventional boiler and chiller providing equivalent heating and cooling ( $E_h$ ,  $E_c$ ) over  $T$  monthly time steps (Equation (2)). The variables used in these calculations are given in Table 1. Cooling delivered from ATEs is assumed to be direct/free cooling, while a heat pump is used for heating. The energy demand profile of the buildings in the model is based on the expected average yearly energy demand of the buildings. It is however corrected for variations in seasons by relative change in daily energy demand according to a time series of temperatures retrieved from KNMI<sup>‡</sup>, as described in [12] and [15].

Table 1. Parameter values used in the simulation study

Parameter	Value or range	Unit	Symbol
ATES nominal temperature difference	4 – 8	[K]	$\Delta T$
ATES pump efficiency	0.25	[-]	$n_p$
Boiler efficiency	0.95	[-]	$\eta_b$
COP chiller	3 – 5	[-]	$COP_c$
COP heat pump	3 – 5	[-]	$COP_{hp}$
Effective flow multiplier	0.4 – 1.0	[-]	$Q_{mult}$
Flow imbalance towards cold wells	-0.2 – 0.2	[-]	$Q_{imb}$
Emission factor (electricity)	0.157	[tCO <sub>2</sub> /GJ]	$f_e$
Emission factor (natural gas)	0.056	[tCO <sub>2</sub> /GJ]	$f_g$
Price for electricity	15 – 60	[€/GJ]	$C_e$
Price for natural gas	5 – 25	[€/GJ]	$C_g$
Distance multiplier between wells	[2.5, 3]	[-]	$d$

<sup>‡</sup> Dutch Institute for Meteorology

$$GHG_{ATES} = \sum_{k=1}^T \sum_{i=1}^N \left( \frac{E_h^{k,i}}{COP_{hp}} + \frac{P^i \cdot c_w}{\eta_p} \cdot \left( \frac{E_h^{k,i} \cdot \frac{(COP_{hp} - 1)}{COP_{hp}} \cdot \Delta t \cdot \Delta T^{k,i} + E_c^{k,i} \cdot \Delta t \cdot |\Delta T^{k,i}|}{Q^{k,i}} \right) \right) \cdot f_e \quad (1)$$

$$GHG_{conv} = \sum_{k=1}^T \sum_{i=1}^N \left( \frac{E_h^{k,i}}{\eta_b} \cdot f_g + \frac{E_c^{k,i}}{COP_c} \cdot f_e \right) \quad (2)$$

The energy costs are calculated similarly to Equations (1) and (2), using energy costs for gas and electricity ( $C_g$  and  $C_e$ ) instead of the corresponding emission factors. A large quantity of simulations with different values for the uncertainty parameter is used, which also includes the pumped volume. To be able to compare the results of the different experiments, the specific GHG savings and cost savings are also determined, Equation (3).

$$S_{GHG} = \frac{GHG_{conv} - GHG_{ATES}}{\bigcup_{i=1}^N V^{sub,i}} \quad \text{and} \quad S_C = \frac{C_{conv} - C_{ATES}}{\sum_{k=1}^T \sum_{i=1}^N (Q^{k,i})} \quad (3)$$

To represent the efficiency with which the subsurface is planned for thermal storage, the  $S_{GHG}$  indicator considers the subsurface volume  $V^{sub}$  which is reserved for each system, i.e. in which new neighbouring wells cannot be created. In addition to physical parameters, this volume is a function of the annual injection volume  $V^i$  for each system, and of the layout parameter  $d$ , Equation (4).

$$V^{sub,i} = \frac{d^2 \cdot V^i \cdot c_w}{c_{aq}} \quad (4)$$

The simulation scenarios will distinguish a baseline permit policy where  $V^i$  is assumed to be a static design value, and an adaptive permit policy where  $V^i$  and  $V^{sub}$  are recalculated periodically according to the effective injection volume (which vary as a function of the  $Q_{mult}$  parameter).

### 2.3. Model setup

This analysis relies on simulation models for ATES adoption and operation which represent the simulated ATES systems in a 2500 m x 2500 m region of the city centre of Utrecht, interacting over a time frame of 300 months. Data for a set of 89 existing and planned wells was obtained from the Utrecht province database, and combined with GIS data to represent building plots and spatial constraints on ATES well location within the NetLogo agent-based environment. The agent-based model assumes that additional new ATES wells are created on the available building plots, within design guidelines on well layout, Figure 4.

The model used to represent the geohydrological setting is a cut-out of the regional MODFLOW [16] groundwater model developed under the authority of the water board Hoogheemraadschap De Stichtse Rijnlanden of district Utrecht. For more details of the model schematization and parameterization is referred to the report of Deltares [17] and TNO [18]. In this section only the main characteristics and the modifications done for this study are discussed.

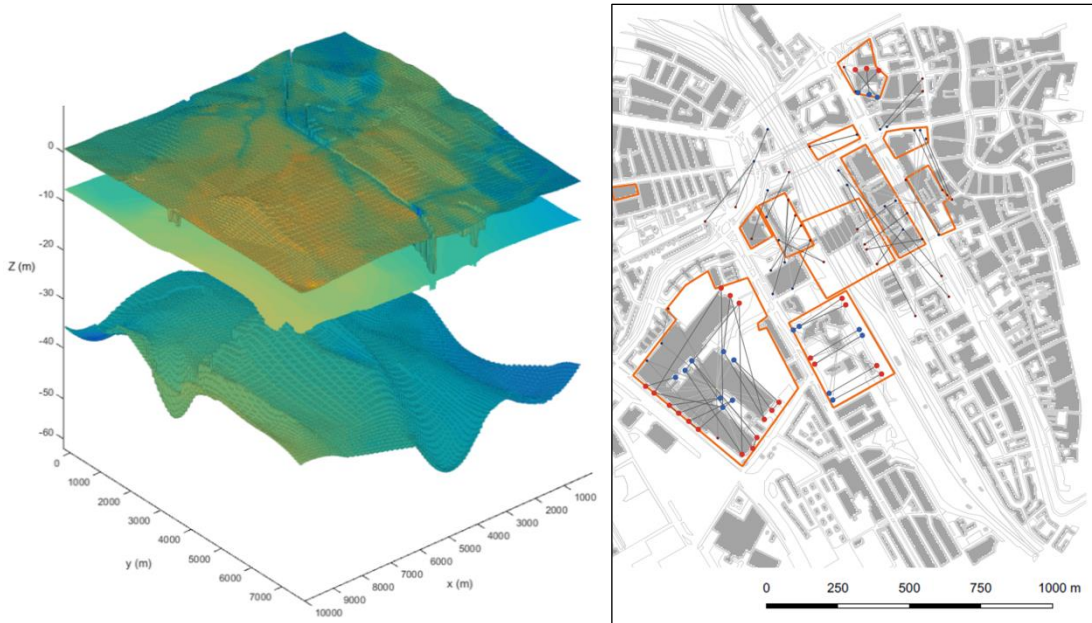


Figure 4. Left: Complete MODFLOW model. Right: Area simulated in the agent-based model, showing building plots available for development (in orange) and ATES wells.

The subsurface of Utrecht is heterogeneous and consists of an alternation of permeable sandy aquifers and non-permeable clayey aquitards. The upper layer is anthropogenic influenced due to excavations and building constructions and therefore strongly mixed [19]. The first (upper) aquifer consists of several horizontal layers, varying from fine sand to gravel, and has a depth from about 4 to 45 m. In the first aquifer ATES systems are placed. A 25 m thick aquitard separates the first from the second aquifer. Faults are present in the original model, but not in the cropped part of model. Constant head boundaries are set up with the corresponding heads from the original model. To minimize running times only relevant processes are simulated, the MODFLOW packages recharge and evaporation (RCH package) and surface runoff (SOF package) are switched off. These packages contain shallow subsurface effects, but as this study focuses on the confined deeper aquifers, these effects can be disregarded without loss of accuracy. The model consists of eight layers, up to about 200 m below surface level. To improve accuracy of the calculated temperature field around the well, the regular grid was refined around the ATES wells.

#### 2.4. Scenarios for ATES layout guidelines and permitting

The spatial planning of ATES systems is usually based on guidelines for the minimal distance between neighbouring wells, which is itself defined as a multiplier ( $d$ ) of the average thermal radius  $R_{th}$  which is the footprint of the thermal cylinder created around the well in the subsurface (illustrated in Figure 5). This value corresponds to the expected radius of thermal influence, based on the analytical solution for heat transport in porous media; the prevailing Dutch guidelines for ATES system design require a distance of  $3 R_{th}$  to avoid thermal interactions. However, these guidelines may be overly conservative [20]. The simulations will therefore test a tighter distance policy of  $2.5 R_{th}$  in addition to the current policy, also see Table 1.



Figure 5. ATES well layout and footprint definition. Thermal radius depends on thermal properties of aquifer and water ( $c_{aq}$ ,  $c_w$ ), storage volume ( $V$ ) and filter screen length ( $L$ )

In addition, Willemsen [6] showed that ATES systems on average only use 40% of their permitted capacity. To evaluate how this “over-claiming” affects total energy savings and individual performance, a multiplier on the theoretical capacity is added to test the effect of smaller effective flows ( $Q_{multi}$  in Table 1).

Furthermore, an adaptive policy measure is evaluated. For the city centre of Utrecht, the permitted volumes of yearly groundwater storage and recovery are obtained from provincial data; starting from this baseline, the simulated permit capacity is adapted every two years based on the actual use of existing ATEs systems. New ATEs systems may be placed in the subsurface space which becomes available from unused claims.

### 3. Results & Discussion

Using the parameters presented in Table 1, 512 experiments were tested for each of the four policy scenarios described in section 2.3: static and adaptive simulated permits, for distances of 2.5 and 3  $R_{th}$ , for a total of 2048 simulations. To illustrate the basic behaviour of the model, Figure 6 shows the envelopes of outcomes for both number of active wells and cost savings, for the different policy scenarios. As can be expected the highest number of wells occur at the adaptive scenarios and the small distance scenarios. Due to the broad uncertainty ranges which were specified, the total cost savings also present a wide distribution.

The tables below summarize sensitivity analysis results for the four main performance indicators, using the Random Forests technique for nonlinear regression to approximate the results of a global sensitivity analysis [21], and showing the five most influential parameters for each output (for values at the end of the simulation). Table 2 shows that the gas price is of crucial importance for the cost savings, while heat pump COP has a smaller impact. The design temperature difference between the wells ( $\Delta T$ ) is significant across the four indicators. As the cost and GHG saving depend directly on the amount of groundwater that is pumped, the volume multiplier ( $Q_{mult}$ ) also has a relative large impact on all performance indicators, especially on GHG savings. Policy is fairly influential on the GHG indicators, but not ranked in the top five most influential variables for economic indicators.

Table 3 summarizes the ensemble results for each policy, from which can be seen that the adaptive policy is performing best except for the specific cost reduction: due to the additional systems which can be built, more groundwater is utilized, resulting in higher overall savings of GHG and costs. However, the additional systems may slightly increase thermal interferences, so that the cost saving per  $m^3$  of groundwater pumped is less. However, the difference across policies on this indicator is relatively minor (<4%), in comparison to the difference on the GHG indicators (12.8% for total GHG savings and 42% on specific GHG savings, due to the greater efficiency in allocation of subsurface volume under the adaptive 2.5  $R_{th}$  policy).

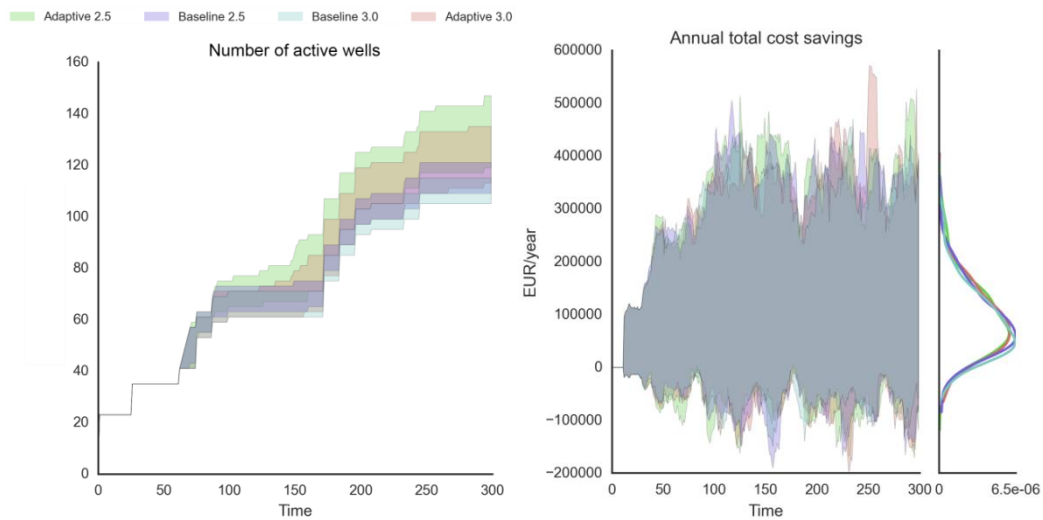


Figure 6. Left: Number of ATEs wells over time across the simulated policies. Right: envelope for total operational cost savings and the density distribution of the solutions

Table 2, Sensitivity of varied parameters for performance indicators

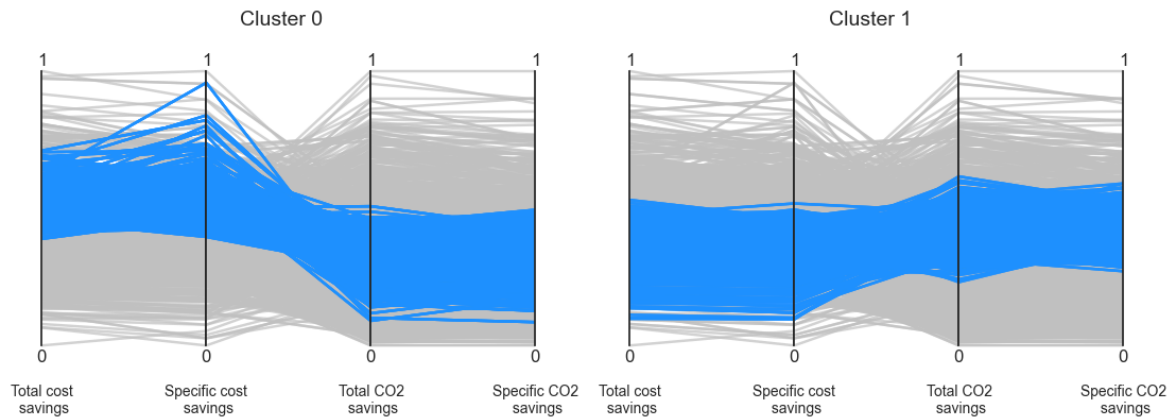
Rank	Total cost savings		Specific cost savings		Total CO <sub>2</sub> savings		Specific CO <sub>2</sub> savings	
	Variable	Estimated importance	Variable	Estimated importance	Variable	Estimated importance	Variable	Estimated importance
1	$C_g$	0.5727	$C_g$	0.6674	$Q_{mult}$	0.4598	$\Delta T$	0.3910

2	$Q_{multi}$	0.1302	$\Delta T$	0.1132	$\Delta T$	0.3851	$Q_{multi}$	0.3336
3	$\Delta T$	0.0965	$C_e$	0.0517	$COP_{hp}$	0.0525	Policy	0.1604
4	$C_e$	0.0474	$COP_{hp}$	0.0451	$COP_C$	0.0492	$COP_{hp}$	0.0478
5	$COP_{hp}$	0.0428	$COP_C$	0.0293	Policy	0.0299	$COP_C$	0.0451

Table 3. Performance indicators for each policy ( $\sigma$ = standard deviation)

Policy	Total cost savings		Specific cost savings		Total CO <sub>2</sub> savings		Specific CO <sub>2</sub> savings	
	Mean (EUR/yr)	$\sigma$	Mean (EUR/m <sup>3</sup> )	$\sigma$	Mean (tCO <sub>2</sub> /yr)	$\sigma$	Mean (kg CO <sub>2</sub> /yr/m <sup>3</sup> )	$\sigma$
Adaptive 2.5 R <sub>th</sub>	96 614	73 576	0.01583	0.0113	3739	1209	0.1316	0.0365
Adaptive 3.0 R <sub>th</sub>	90 017	67 419	0.01579	0.0115	3615	1170	0.1144	0.0322
Baseline 2.5 R <sub>th</sub>	90 127	68 232	0.01613	0.0114	3472	1180	0.1067	0.0362
Baseline 3.0 R <sub>th</sub>	86 152	67 630	0.01638	0.0112	3314	1134	0.0927	0.0317

A scenario discovery approach (e.g. [22]) was used to study the combinations of influential parameters which may cause outcomes of particular interest. A Gaussian mixture model (GMM) was first applied to cluster the simulation experiments across the four performance indicators used in the analysis, using the values at the end of the simulation. This statistical technique assumes that the distribution of outcomes across the 2048 experiments can be approximated by a combination of Gaussian distributions. Using expectation maximization, each of the experiments can then be assigned to one of these distributions. Taking an arbitrary number of four Gaussian components (or clusters), this process resulted in the groups shown in Figure 7. The graphs present the normalized axes used for clustering, so that values of 0 and 1 respectively correspond to the lowest and highest value across the 2048 experiments. For instance, cluster 0 groups experiments which have average total cost savings, relatively high specific cost savings, and relatively low total and specific GHG savings.



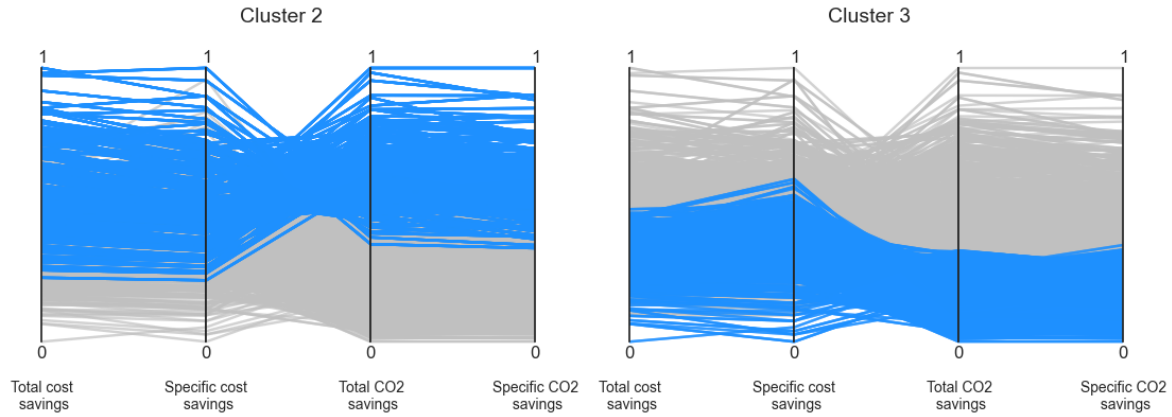


Figure 7. GMM clustering results

These clusters can then individually be studied by using the so-called Patient Rule Induction Method (PRIM) [23] to identify the combinations of uncertainties which tend to lead to a given cluster classification. Cluster 2 (which has relatively high economic performance and the highest CO<sub>2</sub> savings) and Cluster 3 (which has the lowest performance on all indicators) are of particular interest. Table 4 shows the parametric combinations which tend to be associated with these two clusters following the PRIM analysis. The Min./Max. values indicate the parametric ranges identified for each cluster; the p-value estimates the significance of each parameter within this combination using a one-sided binomial test, so that low values indicate a high likelihood that a parametric range is significant in the combination. For each cluster, the PRIM coverage metric gives the fraction of experiments within the cluster which is described by the specified combination of uncertainties; conversely, the PRIM density gives the fraction of experiments which share these combinations which are within the given cluster.

For example, for Cluster 2, this means that 81% of the cases in which  $\Delta T$  is between 6.6 and 8,  $Q_{mult}$  is between 0.79 and 1, the effective COP is between 3.5 and 5, and the planning policy is either adaptive or denser, are classified in the high-performing cluster (although it should be noted the adaptive policies would be less influential with these relatively high values for  $Q_{mult}$ ). Conversely, the results for Cluster 3 show that a combination of low  $\Delta T$ , low  $Q_{mult}$ , low gas price and static or sparser planning policies, tends to cause poor performance. In both clusters, the policies are relatively less significant than the parametric uncertainties.

Table 4. PRIM results for cluster 2 and 3

Parameter	Cluster 2 - Best performance (176 experiments in cluster)			Cluster 3 - Worst performance (546 experiments in cluster)		
	Min.	Max.	p-value	Min.	Max.	p-value
$\Delta T$	6.6	8	~0	4	5.7	~0
$Q_{mult}$	0.79	1	0.002	0.4	0.8	~0
$COP_{hp}$	3.5	5	0.007	-	-	-
$C_g$	-	-	-	5	19	0.008
Policy	[Baseline 2.5, Adaptive 2.5, Adaptive 3.0]		0.047	[Baseline 2.5, Baseline 3.0, Adaptive 3.0]		0.063
PRIM coverage	0.57			0.61		
PRIM density	0.81			0.87		

## 4. Conclusions

The sensitivity results show that economic performance of ATEs systems is dominated by the gas price and two operational factors: the total pumped volume and temperature difference between the wells ( $Q_{mult}$ ,  $\Delta T$ ). This indicates that adaptive/tighter permit policies would not significantly affect operational costs for ATEs users.

This is supported by the mean values for the specific cost savings per unit volume of pumped water, which show a reduction of 3.5% in cost savings for the Adaptive 2.5  $R_{th}$  policy relative to the baseline case. Due to the additional systems created on subsurface volume which would otherwise be reserved, more groundwater is utilized, resulting in higher overall savings of GHG and cost – but slightly reducing the cost savings per m<sup>3</sup> of groundwater pumped. However, the revised policies would have a more significant positive impact on GHG savings, with a 12.8% mean increase in total GHG savings and 42% increase in specific GHG savings per unit of subsurface volume. Heat pump performance is of minor importance for the GHG and cost savings, only for the total GHG savings it is of limited influence.

The results from the scenario discovery showed that the adaptive and denser planning policies perform best, but only when they are also combined with a relatively high permit capacity utilisation. Although this does not follow from the results directly, the better performance of ATES systems using more of their permitted capacity may indicate that an ATES system needs to be substantially sized to contribute significantly to GHG and cost savings, which is in line with literature on heat storage in aquifers [24, 25].

The analysis is limited by some simplifications in operational behaviour of the ATES systems, e.g. the simple heat pump/COP assumptions. The calculation method for assessing energy performance is also relatively straightforward. Therefore it needs to be improved by taking into account a cut-off temperature for cooling, the usage of peak facility for both heating and cooling, and the effect of partial load operation of the heat pump. Because incorporation of these effects will likely only result in a limited change in ATES utilisation, it is expected that these aspects would have a limited effect on the results, but they will be incorporated in the next steps of this research to validate this assumption.

## Acknowledgements

This research was supported by the Netherlands Organization for Scientific Research (NWO) as part of the Uncertainty Reduction in Smart Energy Systems (URSES) research program, under the project Aquifer Thermal Energy Storage Smart Grids (ATES-SG), grant number 408-13-030.

## Nomenclature

$c_{aq}$	=	Specific heat capacity of saturated porous medium; $2.8 \times 10^6$ [J/m <sup>3</sup> /K]
$c_w$	=	Specific heat capacity of water; $4.2 \times 10^6$ [J/m <sup>3</sup> /K]
$C_e$	=	Price for electricity [€/GJ]
$C_g$	=	Price for gas [€/GJ]
$COP_{hp}$	=	COP heat pump [-]
$COP_c$	=	COP chiller [-]
$d$	=	Distance multiplier between wells [-]
$\Delta t$	=	time step [month]
$\Delta T$	=	Temperature difference between extraction and infiltration [K]
$E_h$	=	Energy delivered to the building for heating [J]
$E_c$	=	Energy delivered to the building for cooling [J]
$f_g$	=	Emission factor electricity [tCO <sub>2</sub> /GJ]
$f_e$	=	Emission factor gas [tCO <sub>2</sub> /GJ]
$L$	=	Filter screen length [m]
$\eta_b$	=	Boiler thermal efficiency [-]
$\eta_{th}$	=	Thermal efficiency [-]
$\eta_p$	=	Pump efficiency [-]
$P_p$	=	Power of ATES well pumps [kW]
$Q$	=	Hourly pumping rate of ATES wells [m <sup>3</sup> /hr]
$Q_{imb}$	=	Average flow imbalance towards ATES cold wells [-]
$Q_{mult}$	=	Multiplier on effective annual ATES flow as a fraction of nominal value [-]
$R_{th}$	=	Thermal radius [m]
$T$	=	Temperature [°C]
$V$	=	Injected volume of stored groundwater [m <sup>3</sup> ]

## References

1. Bloemendal, M., T. Olsthoorn, and F. van de Ven, *Combining climatic and geo-hydrological preconditions as a method to determine world potential for aquifer thermal energy storage*. Science of the Total Environment, 2015. **538** ((2015)): p. 621-633.
2. Blum, P., et al., *CO2 saving of ground source heat pump systems – a regional analysis*. Renewable energy 2010. **35**: p. 122-127.
3. Eugster, W.J. and B. Sanner. *Technological status of shallow geothermal energy in Europe*. in *European geothermal congress*. 2007. Unterhaching, Germany.
4. Fry, V.A., *Lessons from London: regulation of open-loop ground source heat pumps in central London*. Quarterly Journal of engineering Geology and Hydrogeology, 2009. **42**: p. 325-334.
5. Verbong, G., et al., *Een Kwestie van Lange Adem. De Geschiedenis van Duurzame Energie in Nederland 1970–2000* 2001, Boxtel: Aeneas.
6. Willemsen, N., *Rapportage bodemenergiesystemen in Nederland*. 2016, RVO / IF technology: Arnhem.
7. CBS, *Issued building permits 1990-2015 retrieved from stailine database*, CBS, Editor. 2016, Central authority for statistics in NL: Den Haag.
8. Ministry-of-Internal-affairs, *Bouwbesluit (Building Act)*. 2012, Ministry-of-Internal-affairs: Den Haag.
9. LGR, *Dutch register/database for groundwater abstractions*, P.o.T. Netherlands, Editor. 2012.
10. NVOE, *Richlijnen Ondergrondse Energieopslag, Design guidelines of Dutch branche association for geothermal energy storage*. 2006: Woerden.
11. Ostrom, E., *Governing the Commons*. 1990, Camebridge: Cambridge University Press.
12. Jaxa-Rozen, M., J.H. Kwakkel, and M. Bloemendal, *The Adoption and Diffusion of Common-Pool Resource-Dependent Technologies: The Case of Aquifer Thermal Energy Storage Systems*, in *PICMET*. 2015: Portland.
13. Dekker, L.d. *Bepalende factoren voor goed functionerende WKO*. 2016; Available from: <http://www.kennisplatformbodemenergie.nl/wp-content/uploads/2015/03/KP3-B3-Bepalende-factoren-voor-goed-functionerende-WKO.pdf>.
14. Kwakkel, J.H., *Exploratory Modelling and Analysis (EMA) Workbench*. 2015.
15. Bloemendal, M., T. Olsthoorn, and F. Boons, *How to achieve optimal and sustainable use of the subsurface for Aquifer Thermal Energy Storage*. Energy Policy, 2014. **66**: p. 104-114.
16. Langevin, C.D., W.B. Shoemaker, and W. Guo, *MODFLOW-2000, the USGS modular groundwater model - Documentation of the SEAWAT-2000 version with variable density flow process and integrated MT3DMS transport process*. 2003, USGS: Tallahassee, Florida.
17. Borren, W., et al., *Ontwikkeling HDSR hydrologisch modelinstrumentarium – HYDROMEDAH. Deelrapport 1: Beschrijving MODFLOW model*. 2009, Deltares: Utrecht.
18. Gunnink, J.L., et al., *Deklaagmodel en geohydrologische parametrisatie voor het beheersgebied van het Hoogheemraadschap "De Stichtse Rijnlanden"*. 2004, TNO: Utercht.
19. Boerefijn, M., et al., *M.e.r. Koude-WarmteOpslag Stationsgebied Utrecht*. 2010, Tauw: Utrecht.
20. Sommer, W., et al., *Optimization and spatial pattern of large-scale aquifer thermal energy storage*. Applied Energy, 2015. **137**: p. 322-337.
21. Breiman, L., *Random Forests*. Machine Learning, 2001. **45**: p. 5-32.
22. Bryant, B.P. and R.J. Lempert, *hinking inside the box: A participatory, computer-assisted approach to scenario discovery*. Technological Forecasting and Social Change, 2010. **77**(34-49).
23. Friedman, J.H. and N.I. Fisher, *Bump hunting in high-dimensional data*. Statistics and Computing, 1999. **9**: p. 123-143.
24. Bloemendal, M. and N. Hartog, *After the boom: Evaluation of dutch ates-systems for energy efficiency*, in *European Geothermal Conference 2016*. 2016, EGEC: Strassbourg.
25. Doughty, C., G. Hellstrom, and C.F. Tsang, *A dimensionless approach to the Thermal behaviour of an Aquifer Thermal Energy Storage System*. Water Resources Research, 1982. **18**(3): p. 571-587.